

Article

Study on the Spatial and Temporal Evolution of NDVI and Its Driving Mechanism Based on Geodetector and Hurst Indexes: A Case Study of the Tibet Autonomous Region

Jian Wang ^{1,2,3,†} , Junsan Zhao ^{1,2,3,*}, Peng Zhou ^{4,5,*} , Kangning Li ^{1,2,3}, Zhaoxiang Cao ⁶ , Haoran Zhang ^{1,2,3}, Yang Han ^{1,2,3}, Yuanyuan Luo ^{4,5} and Xinru Yuan ^{4,5}

¹ Faculty of Land Resources Engineering, Kunming University of Science and Technology, Kunming 650093, China; jian_w@stu.kust.edu.cn (J.W.); likangning@stu.kust.edu.cn (K.L.); zhanghr@stu.kust.edu.cn (H.Z.); hanyang@stu.kust.edu.cn (Y.H.)

² Key Laboratory of Geospatial Information Integration Innovation for Smart Mines, Kunming 650093, China

³ Spatial Information Integration Technology of Natural Resources, Universities of Yunnan Province, Kunming 650211, China

⁴ School of Surveying and Land Information Engineering, Henan Polytechnic University, Jiaozuo 454000, China; yuanyuan@home.hpu.edu.cn (Y.L.); 212204020077@home.hpu.edu.cn (X.Y.)

⁵ State Environmental Protection Key Laboratory of Satellite Remote Sensing, Aerospace Information Research Institute, Chinese Academy of Sciences, Beijing 100101, China

⁶ College of Marine Sciences, Shanghai Ocean University, Shanghai 201306, China; m210200599@st.shou.edu.cn

* Correspondence: junsanzhao@netease.com (J.Z.); 212104020091@home.hpu.edu.cn (P.Z.)

† These authors contributed equally to this work.

Abstract: The Tibet Autonomous Region (TAR) is located in the mid-latitude and high-cold regions, and the ecological environment in most areas is fragile. Studying its surface vegetation coverage can identify the ecosystem's development trends and provide a specific contribution to global environmental change. The normalized difference vegetation index (NDVI) can better reflect the coverage of surface vegetation. Therefore, based on remote sensing data with a resolution of 1 km², air temperature, precipitation, and other data in the same period in the study area from 1998 to 2019, this paper uses trend analysis, F-significance tests, the Hurst index, and the Geodetector model to obtain the spatial distribution, change characteristics, and evolution trends of the NDVI in the TAR in the past 22 years. At the same time, the quantitative relationship between natural and human factors and NDVI changes is also obtained. The study results show that the NDVI in the southern and southeastern parts of the TAR is higher, with mean values greater than 0.5 showing that vegetation cover is better. The NDVI in the western and northwestern parts of the TAR is lower, with mean values less than 0.3, indicating vegetation cover is worse. NDVI in the TAR showed an overall increasing trend from 1998 to 2019 but a decreasing trend in ridgelines, snow cover, and glacier-covered areas. The areas where NDVI values show a trend of increasing and then decreasing in the future account for 53.69% of the total area of the TAR. The most crucial factor affecting NDVI changes in the TAR is soil type, followed by influencing factors such as vegetation cover type, average annual air temperature, and average annual precipitation. The influence of natural elements is generally more significant than anthropogenic factors. The influencing factors have synergistic effects, and combining anthropogenic factors and other factors will show mutual enhancement and non-linear enhancement relationships. This study provides a theoretical basis for natural resource conservation, ecosystem restoration, and sustainable human development strategies in the TAR.

Keywords: normalized difference vegetation index (NDVI); spatial-temporal distribution characteristics; Hurst index; Geodetector; meteorological and social factors; soil and land use types



Citation: Wang, J.; Zhao, J.; Zhou, P.; Li, K.; Cao, Z.; Zhang, H.; Han, Y.; Luo, Y.; Yuan, X. Study on the Spatial and Temporal Evolution of NDVI and Its Driving Mechanism Based on Geodetector and Hurst Indexes: A Case Study of the Tibet Autonomous Region. *Sustainability* **2023**, *15*, 5981. <https://doi.org/10.3390/su15075981>

Academic Editors: Xin Huang, Jiayi Li, Xian Guo and Dawei Wen

Received: 24 January 2023

Revised: 21 March 2023

Accepted: 23 March 2023

Published: 30 March 2023



Copyright: © 2023 by the authors. Licensee MDPI, Basel, Switzerland. This article is an open access article distributed under the terms and conditions of the Creative Commons Attribution (CC BY) license (<https://creativecommons.org/licenses/by/4.0/>).

1. Introduction

As a producer of the terrestrial ecosystem, vegetation is closely related to natural environmental elements such as climate, soil, topography, and water resources [1]. It plays a crucial role in water conservation [2], soil erosion prevention [3], wind and sand control [4], and ecosystem stability [5]. Therefore, studying vegetation cover in different areas is crucial for ecological conservation in the region. Previous studies on the ecological aspects of western China have focused on large areas such as the Tibetan Plateau and the Taklamakan Desert. Still, to further study the characteristics of the local ecological environment in these areas, targeted studies are needed in Tibet and Qinghai.

Because of the advantages of remote sensing technology tools, such as extensive range, the ability to analyze long time series, and high resolution, they have become essential for studying the ecological environment. Among them, the normalized difference vegetation index (NDVI) can accurately respond to the status of surface vegetation cover and is thus widely used to evaluate vegetation growth and development and ecological environment changes [6]. Previous studies on NDVI changes and drivers using trend analysis, correlation analysis, or partial correlation analysis have been conducted in different regions, including globally, across Europe, in Asia, in China, in the Yangtze River Basin, in the Yellow River Basin, and in the Qinghai–Tibet Plateau [7–12]. These methods have achieved good results; however, they still need to meet the needs of the current research stage. The Geodetector model proposed by Wang [13] et al. bridges the gap between the correlation analysis methods used in previous studies. The technique has a greater advantage over other methods in quantifying the relationship between the NDVI and related drivers [14]. For example, Gao [15] et al. found that the Geodetector model could better reflect the spatial heterogeneity of vegetation cover and quantify the drivers of vegetation change and the interactions between individual factors in their study of vegetation cover in the Sanjiangyuan region. Wu (2022) et al. [16] used Geodetector to examine the spatial and temporal variability in the NDVI and its dual response to climate change and human activities in three northeastern provinces of China.

Vegetation restoration is one of the most effective ways to improve the ecological environment and control soil erosion. Therefore, monitoring and predicting vegetation cover is significant to regional ecological restoration and environmental management. However, in the past, scholars mostly used Markov chains [17] or empirical function models [18] to predict vegetation cover, and although their results are scientific, they are less generalizable. The Hurst index is different from the traditional prediction models as it is an important indicator that describes the long period of non-function. It can detect the existence of ultra-long periodicity in a time series; thus, the Hurst index can be used to predict the future growth of vegetation. For example, Han [19] used the Hurst index to predict the future based on the current vegetation growth trend in the region, and Zhang [20] predicted future vegetation growth in the Qinba Mountains.

To study the characteristics of the local ecological environment of the Tibetan Plateau in western China and refine the driving mechanisms behind the local ecological environment, the TAR was selected for this paper. The TAR is located in the southwestern part of the Tibetan Plateau, a region with complex soil types, diverse land use types, and rich vegetation types, making studying vegetation conservation in the TAR extremely important. From a review of previous studies, we found that earlier studies on the characteristics of vegetation cover change in the TAR have used short time series or lower-resolution datasets. Thus, their results have varied [21–23]. Meanwhile, previous studies on the factors influencing the NDVI in the TAR have focused on air temperature and precipitation. These studies needed to consider essential factors affecting vegetation growth, such as soil and land use types. They needed more research on anthropogenic factors and the interaction between anthropogenic and natural factors [24]. In addition, studies on predicting future growth trends in the TAR have often used traditional mathematical and physical models [25–29]. Therefore, integrated trend analysis, Geodetector, and Hurst indices can better provide a more detailed analysis of the local ecological environment.

The response of plateau ecosystems to global climate change is obvious, but the fragile environment in which plateau vegetation grows is highly vulnerable to damage by natural and anthropogenic factors. Therefore, the purposes of this paper are as follows: to analyze the evolution of the NDVI in the TAR between 1998 and 2019 using one-dimensional linear regression and F-significance tests; to quantitatively study the significant effects of natural and anthropogenic factors on the NDVI and their interactions on the NDVI with the help of Geodetector; and to make reasonable predictions of future vegetation growth trends using the Hurst index. These studies are intended to provide ecological and environmental protection departments with a scientific basis and reference for decision making in vegetation conservation and the formulation of relevant policies.

2. Material and Methods

2.1. Study Area

The TAR (located between 26°50′ and 36°53′ north latitude and 78°25′ and 99°06′ east longitude) is located on the southwestern border of China and the southwestern part of the Qinghai–Tibet Plateau; it covers an area of 1,228,400 square kilometers and is adjacent to Xinjiang, Yunnan, and India. The TAR has a significant air temperature difference between day and night, and precipitation gradually decreases from southeast to northwest. Its many landscapes include snow-capped mountains, glaciers, deserts, grasslands, and primeval forests. In addition, most parts of the TAR are characterized by low vegetation cover and sparse population density.

2.2. Data

China's annual normalized difference vegetation index (NDVI) data were obtained from the Resource Environment Science Data Registration and Publication System (<http://www.resdc.cn/>, accessed on 10 December 2021) with a spatial resolution of 1 km. In this paper, NDVI data, such as classification and merging, were preprocessed to obtain vegetation data with a spatial resolution matching the climate factors. The digital elevation model (DEM) is derived from the geospatial data cloud (<http://www.gscloud.cn/>, accessed on 26 December 2021) with a spatial resolution of 30 m, which is used to calculate the slope and aspect data. The average monthly air temperature data were obtained from the National Earth System Science Data Center shared platform (<http://www.geodata.cn/>, accessed on 26 December 2021) with a spatial resolution of 0.0083333° (about 1 km). The NASA Data Center provided month-by-month precipitation data (<https://disc.gsfc.nasa.gov/>, accessed on 26 December 2021). Land use data were obtained from the Resource Environment Science and Data Center (<https://www.resdc.cn/>, accessed on 28 January 2022). Soil type data were obtained from Nanjing Soil Institute, Chinese Academy of Sciences. Vegetation cover data were obtained from the Cold and Dry Zone Science and Data Center (westdcwestgis.ac.cn, accessed on 30 January 2022). Gross regional product data were received from China Knowledge Network (<http://data.cnki.net/Yearbook/>, accessed on 20 April 2022). Population density data were obtained from East View Cartographic (<http://landscan.ornl.gov/>, accessed on 20 April 2022).

2.3. Methods

2.3.1. Data Preprocessing

Figure 1 shows the study methodology. In the data collection and processing phase, we obtained NDVI images for each year from 1998 to 2019 through maximum synthesis to obtain vegetation cover maps. We processed the climate factor data through resampling to derive air temperature and precipitation data consistent with NDVI resolution. In addition, the DEM data were processed with the help of ArcGIS(10.8) software to obtain elevation, slope, and aspect data. Soil types and land use types have also been reclassified. There is also the gross regional product, which matches areas in ArcGIS software.

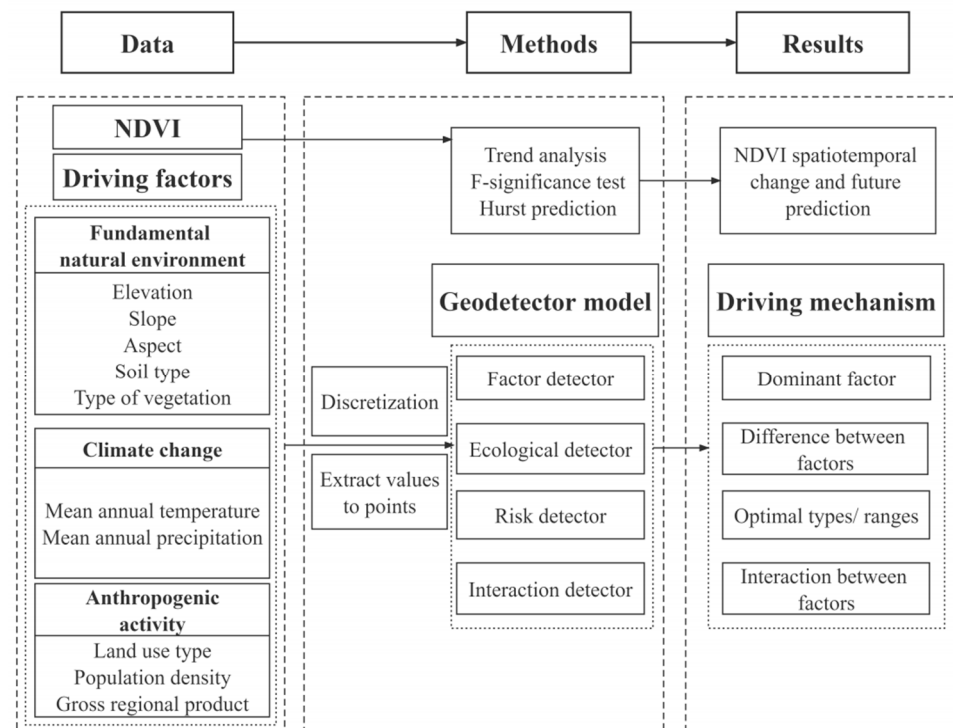


Figure 1. The methodology framework of this study.

2.3.2. Spatial Trend Analysis Method

First, we used one-dimensional linear regression analysis and least squares to fit the remote sensing images from 1998 to 2019. The NDVI slope within each raster was statistically performed to obtain the multi-year trend in NDVI changes to comprehensively analyze the direction and rate of multi-year vegetation cover change in the TAR. The equation is as follows:

$$\text{slope} = \frac{n \times \sum_{i=1}^n x_i y_i - (\sum_{i=1}^n x_i)(\sum_{i=1}^n y_i)}{n \times \sum_{i=1}^n x_i^2 - (\sum_{i=1}^n x_i)^2} \quad (1)$$

where y_i is the value of year x_i ; when slope > 0 , there is an increasing trend, and when slope < 0 , there is a decreasing trend.

2.3.3. F-Test Method

To further evaluate the status of vegetation cover change, the F-test method was used to analyze the significance of the NDVI change trend, which was used to indicate the confidence level in the trend change.

$$a = \bar{y} - (\text{slope} * \bar{x}) \quad (2)$$

where a is the intercept, \bar{y} is the 22-year NDVI mean, and \bar{x} is the annual standard.

$$F = \sum_{i=1}^n (\tilde{y}_i - \bar{y}) \times \frac{n-2}{\sum_{i=1}^n (y_i - \tilde{y}_i)^2} \quad (3)$$

where n is the study time series, \tilde{y}_i is the fitted regression value, \bar{y} is the mean of n years, and y_i is the value of year x_i .

2.3.4. Hurst Predictive Analytics

The Hurst index was initially proposed by the British hydrologist Harold Edwin Hurst and named after him. In his study of the relationship between water flow and

storage capacity in the Nile's reservoirs, he found that fractal Brownian motion was a good description of the long-term storage capacity of the pools. Flood processes are time series curves with a long memory associated with time. The longer the drought, the more likely there will be a sustained drought; larger floods will still occur after a significant flood year. The Hurst index is based on Hurst's long-term hydrological observations of the Nile, and this basis is proposedly established by rescaled polar difference (R/S) analysis. The Hurst index has three forms: 1. If $H = 0.5$, it indicates that the time series can be described by random wandering. 2. If $0.5 < H < 1$, it indicates the existence of long-term memory in the time series. 3. If $0 \leq H < 0.5$, it indicates pink noise (anti-continuity), i.e., a mean reversion process. As long as $H \neq 0.5$, the time series data can be described by biased Brownian motion (fractal Brownian motion).

2.3.5. Geodetector

Geodetector is a statistical tool to detect spatial heterogeneity and its driving factors. It reveals the impact of geographical and environmental factors on geographical phenomena through four sensors: risk detection, factor detection, ecological detection, and interactive detection. Geodetector is collinear and immune to multiple independent variables and does not require correlation analysis of variables to be conducted.

The steps for using Geodetector are divided into two parts. The first step is collecting and processing data; the collected data consists of a dependent variable Y and an independent variable X . The independent variable is a type quantity (e.g., air temperature or precipitation). The independent variables selected in this paper have been converted into numerical quantities in the experiments. The quantitative values have been discretized and applied to the calculation of the Geodetector model. The second step is the software readout; the specific operations are shown below.

Factor Detection

A factor detector was used to measure the magnitude of the determining power of natural and anthropogenic factors on the spatial distribution of the NDVI in the TAR, and the specific explanatory power of the elements was portrayed by q -values.

$$q = 1 - \frac{\sum_{h=1}^L N_h \sigma_h^2}{N \sigma^2} = 1 - \frac{SSW}{SST} \quad (4)$$

$$SSW = \sum_{h=1}^L N_h \sigma_h^2 \quad (5)$$

$$SST = N \sigma^2 \quad (6)$$

where $h = 1$ and L is the classification of independent variable Y or factor X . N_h and N are the number of units in category h and the whole region, respectively. σ_h^2 and σ^2 are the variance of Y values in category h and the entire region, respectively. SSW is the sum of the internal conflicts of the categories, and SST is the total variance of the whole area. The value range of q is 0~1. The higher the value of q , the greater the factor's influence on NDVI spatial differentiation.

Interaction Detection

Interaction detection allows for identification of the interaction of different natural and anthropogenic factors on the spatial distribution of the NDVI in the TAR. In addition, it also assesses whether the mutual interaction between the factors increases or decreases the explanatory power of the spatial distribution of the NDVI and whether the effects of these factors on the spatial distribution of the NDVI in the TAR are independent. Interaction detection was performed by calculating the q -value ($q(X1 \cap X2)$) of any factors $X1$ and $X2$ superimposed separately to determine whether and to what extent there was an interaction between the elements. The interaction between them is shown in Table 1.

Table 1. Analysis of the interaction between NDVI and different factors.

Judgment Basis	Interaction
$q(X_1 \cap X_2) < \min(q(X_1), q(X_2))$	Non-linear weakening
$\min(q(X_1), q(X_2)) < q(X_1 \cap X_2) < \max(q(X_1), q(X_2))$	Single-factor nonlinear attenuation
$q(X_1 \cap X_2) > \max(q(X_1), q(X_2))$	Two-factor enhancement
$q(X_1 \cap X_2) = q(X_1) + q(X_2)$	Mutual independence
$q(X_1 \cap X_2) > q(X_1) + q(X_2)$	Non-linear enhancement

Ecological Detection

Ecological detection is used to assess whether there is a significant difference between the two factors on the spatial distribution of the NDVI in the attribute TAR and is measured by F statistics:

$$F = \frac{N_{x_1}(N_{x_2} - 1)SSW_{x_1}}{N_{x_2}(N_{x_1} - 1)SSW_{x_2}} \quad (7)$$

$$SSW_{x_1} = \sum_{h=1}^{L_1} N_h \sigma_n^2 \quad (8)$$

$$SSW_{x_2} = \sum_{h=1}^{L_2} N_h \sigma_n^2 \quad (9)$$

where N_{x_1} and N_{x_2} denote the sample sizes of the two factors X_1 and X_2 , respectively. SSW_{x_1} and SSW_{x_2} denote the sum of the internal variances of the strata in the stratification formed by X_1 and X_2 , respectively, and L_1 and L_2 represent the number of variable X_1 and X_2 strata, respectively. Where the null hypothesis $H_0: SSW_{x_1} = SSW_{x_2}$. Suppose H_0 is rejected at the significance level of α . In that case, this indicates significant differences in the effects of the two factors X_1 and X_2 on the spatial distribution of the NDVI in the attribute TAR.

Risk Detection

The risk detector analyzed each factor partition's high- and low-value areas. The t -test was used to test whether there was a significant difference ($p < 0.05$) between the NDVI values of different sections of each factor. That is, it is possible to know whether there is a substantial difference in the effect of independent variables on the spatial distribution of the NDVI.

In summary, use of the Geodetector tool can determine the relationship between the spatial distribution of NDVI vegetation and the spatial distribution characteristics of the influencing factors; that is, if a factor drives change in the NDVI, then the spatial distribution of the NDVI will be similar to the spatial distribution of that factor. This method has now been successfully used to study the drivers of NDVI change.

3. Results

3.1. Characteristics of Time Dimensional NDVI Changes

Based on the obtained NDVI data, the average NDVI values from 1998 to 2019 were calculated. Since the value of the NDVI is between 0 and 1, it is not easy to visually observe the changing trend. The NDVI mean value obtained was expanded 10,000 times in the experiment, and the results are shown in Figure 2. The NDVI of the TAR from 1998 to 2018 showed a fluctuating upward trend, increasing at a rate of 0.002 per year; however, there were differences in the NDVI's growth rate in different periods. The annual average value of the NDVI is 0.305, and the difference between the maximum and minimum values is 0.052; the value of the NDVI shows an increasing trend year by year from 1998 to 2018, which can indicate that the TAR has had good results in terms of vegetation protection over the last 22 years. We also found that vegetation recovered faster in the years after 2010. On the one hand, we found that average annual air temperature and precipitation had

improved considerably since 2010 compared to the pre-2010 period, making it more suitable for vegetation growth. On the other hand, during this period, the Chinese government paid more attention to ecological protection, establishing a large number of natural ecological reserves throughout the country, planting trees in arid areas, preventing wind and reducing sand, and improving the vegetation growth environment in the TAR, which led to an increase in the rate of vegetation recovery.

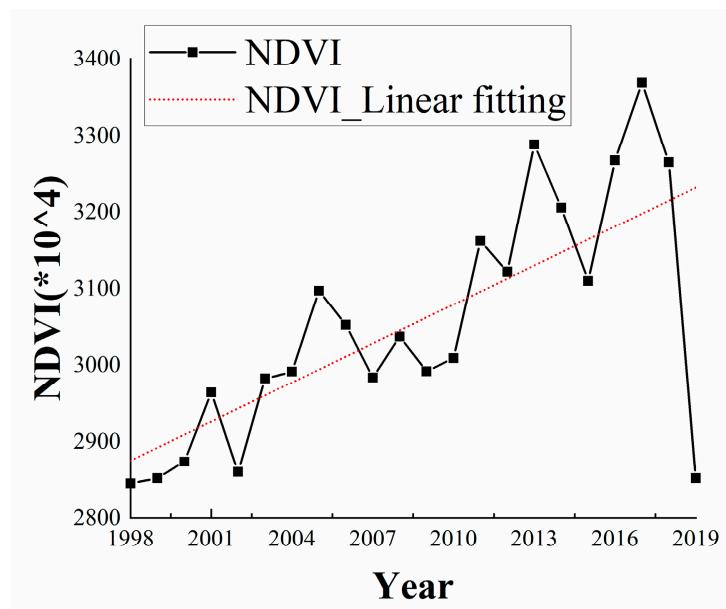


Figure 2. The near linear trend of the NDVI in the TAR (1998–2019).

Combining Figures 2 and 3, we can see that after a fluctuation in average annual air temperature and average annual precipitation in the Tibet Autonomous Region from 1998 to 2019, the NDVI value of the following year will also fluctuate. As shown in Figure 1, the NDVI in 2019 showed a definite downward trend. Corresponding to Figure 2, we find that average annual air temperature and average annual precipitation in the Tibet Autonomous Region also showed a precipitous decrease from 2017 to 2018. To ensure the preciseness of the experiment, we also checked the natural disaster yearbooks of Tibet in 2019 and 2020. In the yearbooks, we found that landslides occurred successively in Jiangda County of Changdu City and Milin County of Linzhi City in October 2018, blocking the Jinsha River and the Yarlung Zangbo River and forming barrier lakes. From December 17th to 19th, due to the joint influence of the cloud system around the periphery of tropical storm “Petai” in Bangladesh moving northward and the cold air in the north moving southward, slight to moderate snow generally occurred in cities other than Ali. Some places experienced heavy snow, with significant cooling after the snow. These sudden factors are also important factors leading to a sharp decline in the NDVI value in 2019.

Through research in this area, we believe that air temperature and precipitation are key factors affecting vegetation growth. The effect of air temperature and precipitation on vegetation growth lags in the time dimension.

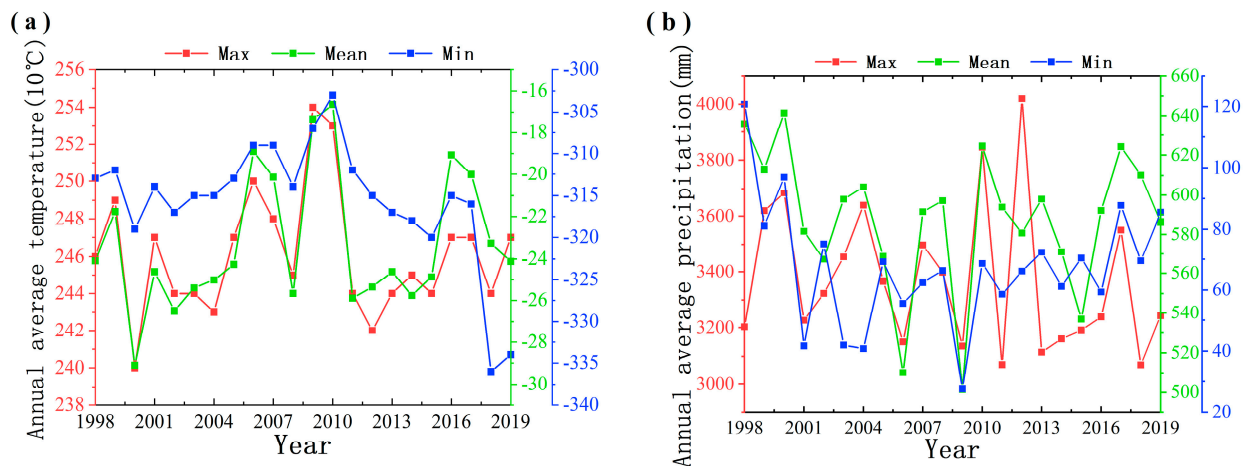


Figure 3. Change trend of average annual air temperature (a) and average annual precipitation (b) (1998–2019).

3.2. Spatial Dimensional Variation Characteristics of the NDVI

By studying the change characteristics of the NDVI in the time dimension, we found that the NDVI values in the TAR showed a gradual increase from 1998 to 2019. To clarify the variation in NDVI values in each region, we also analyzed the variation characteristics of the NDVI through the spatial dimension.

Firstly, vegetation cover in the TAR is divided into five categories: low vegetation cover areas (≤ 0.1), medium–low vegetation cover areas (0.1–0.3), medium vegetation cover areas (0.3–0.5), medium–high vegetation cover areas (0.5–0.7), and high vegetation cover areas (≥ 0.7), which account for 9.89%, 55.83%, 13.75%, 11.77%, and 8.75%, respectively. As shown in Figure 4, the highest coverage area in the TAR is in the Linzhi area, followed by the Lhasa, Shannan, and Changdu areas; the NDVI value of the TAR as a whole decreases from southeast to northwest, and the low vegetation coverage areas are mainly distributed in the northern TAR and northwestern TAR.

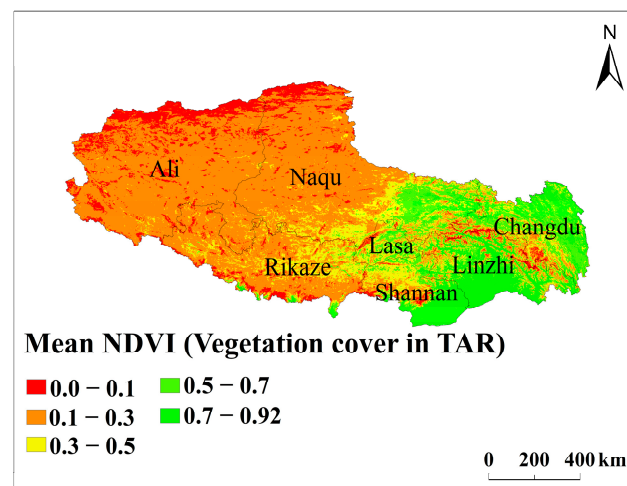


Figure 4. Vegetation coverage in the TAR.

Secondly, trend regression analysis was used to analyze the trends in NDVI from 1998 to 2019 on the pixel metric-scale for research, and the results are shown in Table 2 and Figure 4. The regions with increasing NDVI trends accounted for 54.63% of the whole region, and those with decreasing NDVI trends accounted for 13.93%, with a clear difference

between the two; the areas with significantly increasing NDVI values were mainly located in the southeastern TAR (Linzhi, Changdu, and Shannan).

Table 2. Results of change trends in the study area as a percentage.

Trends	The Proportion	The Proportion of the Total Area of the Study Area (%)
Severe degradation	< -0.005	1.95%
Slight degradation	$-0.005 - 0.001$	11.98%
No change	$-0.001 - 0.001$	31.44%
Slight improvement	-0.004	33.85%
Significant improvement	> 0.004	20.78%

This paper also finds a severe trend of vegetation degradation in glaciated, snow-covered areas and the Himalayas. Combining the topographic and landscape data shows that the northwestern Tibetan region, as well as the Himalayas, is higher in altitude with a landscape type of snow-covered mountains and bare rock, while the landscape type in the Ali region consists of raw land, desert, and some grassland. Although the vegetation cover in these areas is very sparse and difficult to draw attention to, the vegetation in these areas is sensitive to climatic changes and human damage. It is therefore necessary to analyze the specific factors influencing vegetation cover in Tibetan areas by considering factors such as air temperature, precipitation, altitude, and the type of ground cover.

As can be seen from Figures 5 and 6, the spatial distribution of average annual precipitation and average annual air temperature is similar to the spatial distribution of the NDVI, showing a gradually decreasing trend from southeast to northwest. The spatial distribution of average annual air temperature coincides more closely with the spatial distribution of the NDVI. In the southeastern part of the study area, the average annual air temperature and average annual precipitation are numerically higher in the Linzhi, Shannan, and Changdu areas, with the average annual air temperature remaining above 0°C and the average annual precipitation remaining around 750 mm. The NDVI is generally greater than 0.5, which is more suitable for plant growth than other areas; therefore, the NDVI value increases significantly. In the glaciated, snow-covered, and Himalayan regions, average annual precipitation and average annual air temperature are relatively low, with average annual air temperatures remaining below 0°C , average annual precipitation below 750 mm, and sparse vegetation cover, thus resulting in a slowly increasing trend in NDVI values in this part of the region.

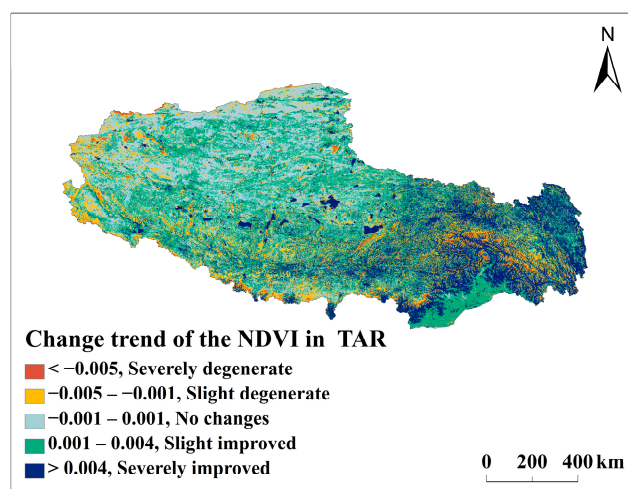


Figure 5. Significant change trend of the NDVI in the TAR (1998–2019).

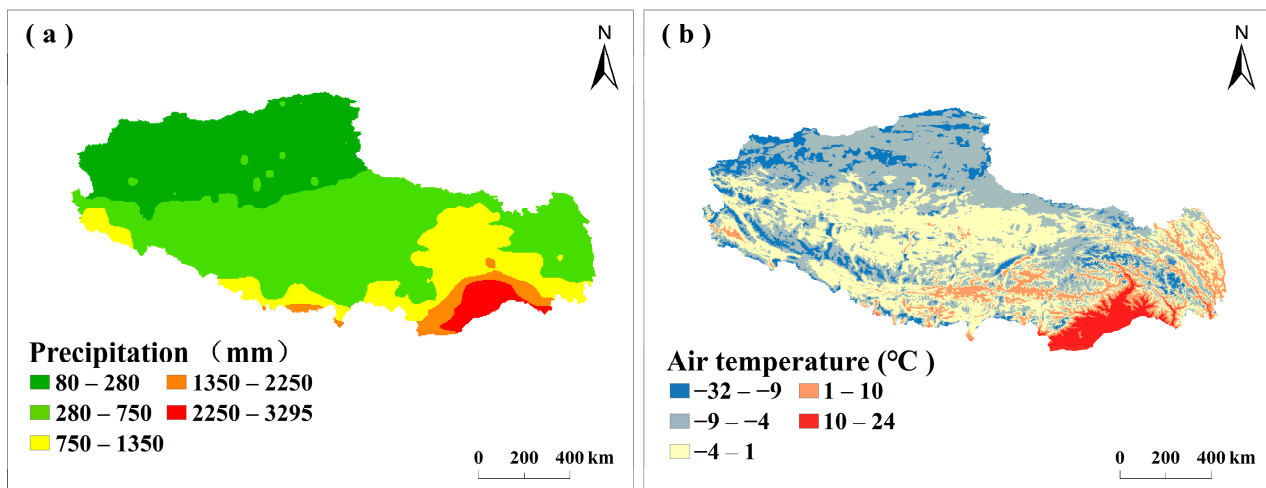


Figure 6. Precipitation (a) and air temperature (b) in the TAR (1998–2019).

This shows that precipitation and air temperature are important factors affecting plant growth in the study area, which is consistent with the results of Wei [30] et al. on the response of the NDVI to climate change across the Chinese region.

3.3. F-Significance Test and Hurst Prediction

The study in Sections 3.1 and 3.2 found that the high NDVI areas in the study area were mainly distributed in the southeast Tibetan region, and the overall NDVI trend showed an increasing trend. To further understand the direction of the NDVI and the future evolution of vegetation in the study area, this study uses the F-significance test and the Hurst index to conduct the following study.

The results of the F-significance test are shown in Figure 7a. The NDVI showed an overall increasing trend, with a 72.56% increase and a 42.13% significant increase; 27.44% of the area showed a reduction and 7.25% a significant reduction. Sites with a significant increasing trend in NDVI were much larger than areas with a decreasing trend. The significantly decreasing areas are mainly found in the snow-capped mountains, permanent ice sheet areas, and the Himalayas. Combined with Figure 3a, it can be seen that the average annual air temperature in the TAR increased from 1998 to 2019 relative to the previous period, and the melting of permafrost caused by the increase in air temperature caused soil moisture loss in areas with higher slopes, which in turn led to a reduction in the NDVI for moisture-sensitive plants (e.g., meadows). At the same time, there is no significant decrease in vegetation in the central part of the TAR or other mountain ranges. As shown in Figures 4, 5 and 7a, the increasing trend in NDVI far exceeds the decreasing trend, which may result from the gradual change in climatic and social factors in this part of the region toward proper vegetation growth. The construction of ecological projects in this area has also had a favorable impact on vegetation growth, resulting in a significant increase in NDVI.

In addition, the spatial distribution map was calculated using the Hurst index for the NDVI of the TAR from 1998 to 2019 (Figure 7b). From the figure, it can be seen that the Hurst index ranges from 0.11065 to 0.86367, which meets the prediction criteria. A Hurst index of less than 0.5 and greater than 0 accounted for 72.06% of the area, and the region greater than 0.5 accounted for 27.94% of the area. This result indicates a definite inverse trend in the future change of NDVI in the TAR. The future vegetation growth trend in 72.06% of the area improves before returning to the original state.

Finally, the results of the F-significance test and the Hurst index superimposed on the analysis are shown in Table 3, which indicate that the future changes in NDVI values in the TAR will mainly increase continuously. However, about 8.1% of the area shows a continuous decreasing trend, primarily in the snow-capped regions of the TAR.

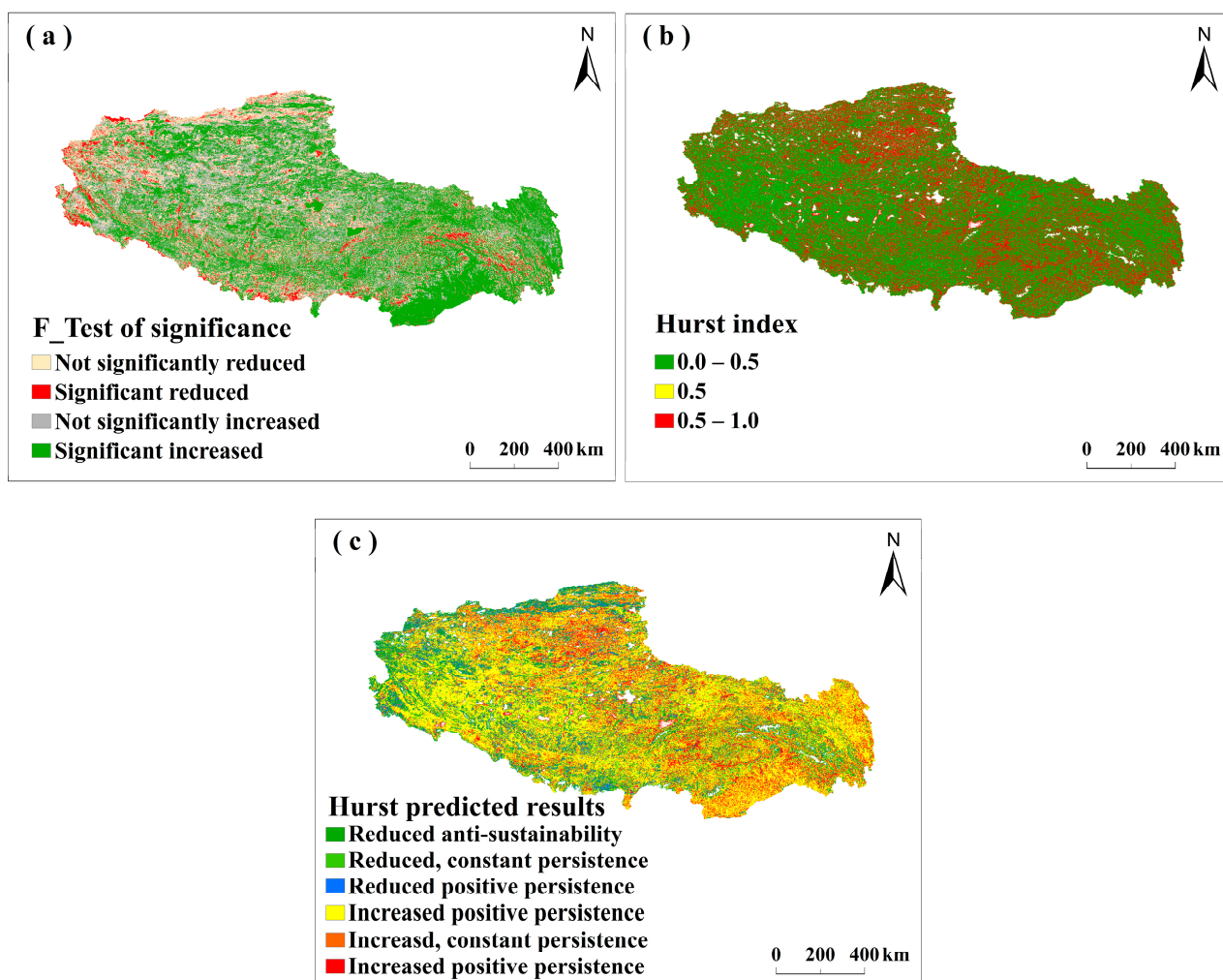


Figure 7. F-significance test (a), Hurst index (b), and Hurst branch predictor (c) (1998–2019).

Table 3. Table of trends (Hurst-predicted).

Level	Percentage (%)
Decrease and Anti-Continuity	18.37
Decrease and Persistence Constant	0
Decrease and Positive Persistence	8.1
Increasing and Anti-Continuous	53.69
Increasing and Persistent	0
Increasing and Positive Persistence	19.88

3.4. Geodetector Analysis

Based on the findings in Sections 3.1 and 3.2, we can find that the spatial distribution of the NDVI shows a robust spatial differentiation. To investigate the reasons for the spatial differentiation of vegetation, we collated the driving mechanisms of soil type, land use, and other factors related to vegetation change in the TAR for further study. As shown in Figure 8, the spatial distribution of our selected drivers is similar to the spatial distribution of vegetation in the study area (Figure 5). In this section, we used the Geodetector model to further analyze the spatial variation in NDVI values and the drivers of the NDVI to reveal the interactions between the various factors and their effects on NDVI change.

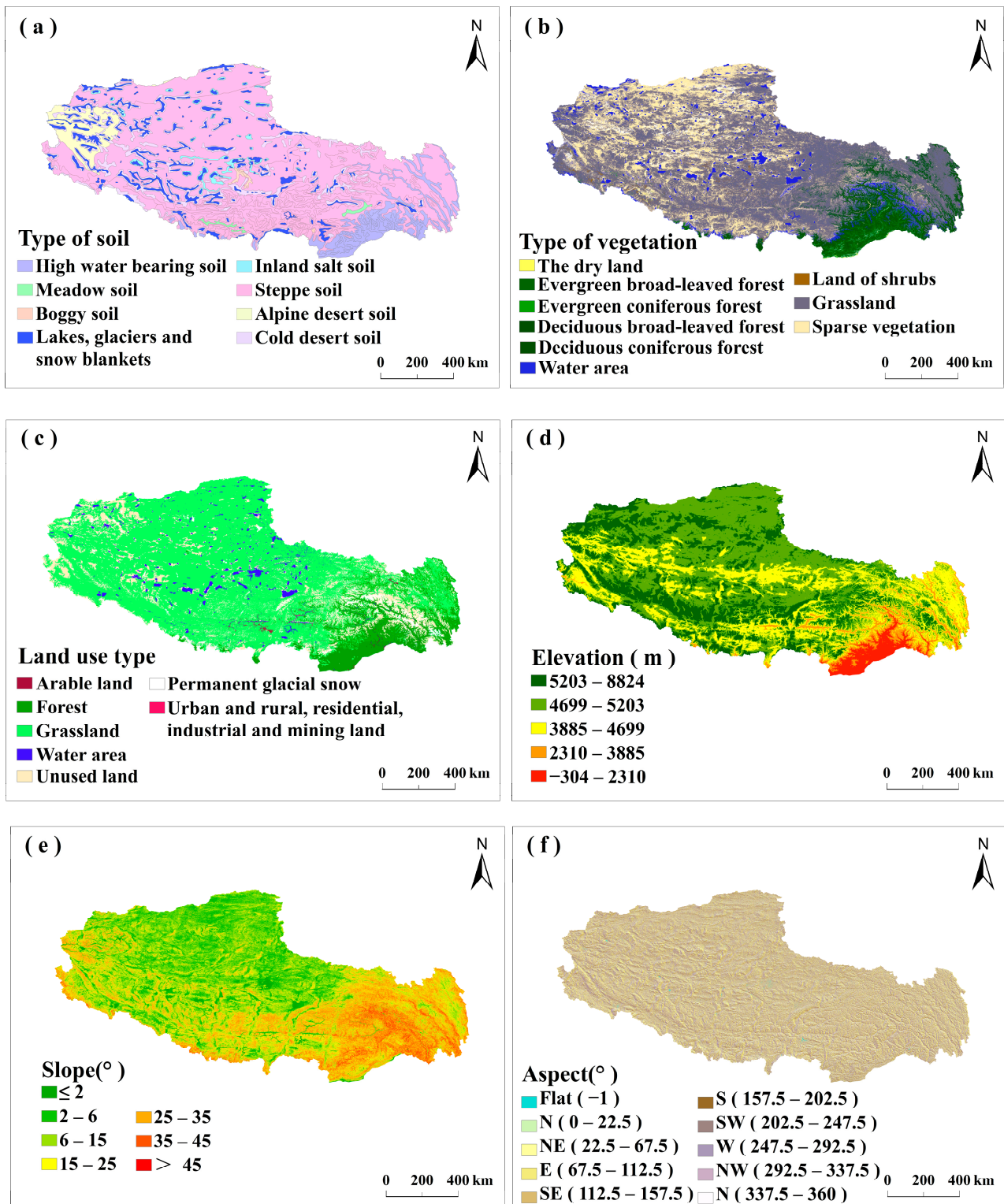


Figure 8. Cont.

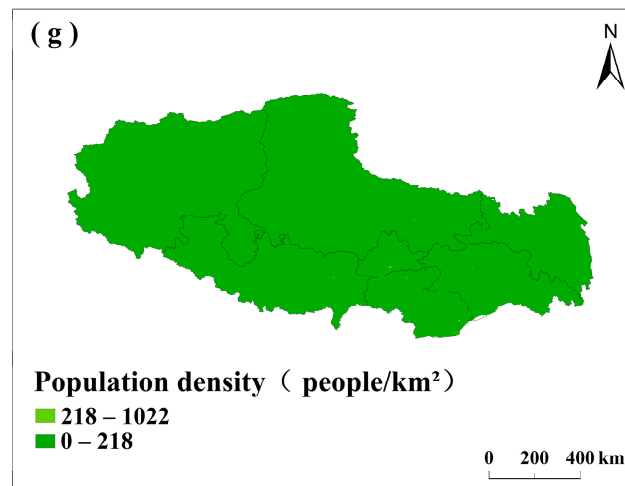


Figure 8. Factors: type of soil (a), type of vegetation (b), land use type (c), elevation (d), slope (e), aspect (f), population (g).

Using the previous trend analysis results and the F-significance test, 2000, 2005, 2010, and 2015 were set as the characteristic years. Soil type, vegetation cover type, slope, slope orientation, DEM, average annual air temperature, average annual precipitation, land use, gross regional product, and population density were selected as the driving factors of the vegetation index in the TAR (Table 4). The significance of the influence of a single element on NDVI values and the result of the interaction between factors on NDVI values were analyzed with the help of the Geodetector model. The results are as follows:

Table 4. Factors analysis.

Stability Factor	Soil type	X1
	Vegetation type	X2
	Slope	X3
	Aspect	X4
	DEM	X5
Change factor	Average annual air temperature	X6
	Average annual precipitation	X7
	Land Use	X8
	Gross regional product	X9
	Population Density	X10

3.4.1. Interaction Analysis

The results of data detection in the year 2000 are shown in Table 5. It was found that the interaction detection results of slope orientation (X4) with soil, vegetation cover type, slope, DEM, average annual air temperature, average annual precipitation, land use type, gross regional product, and population density all showed non-linear enhancement. The results of the interaction detections for the other factors are all bivariate enhancements. In 2005 and 2010, Geodetector interaction detections are consistent with the 2000 interaction detections. However, in the 2015 treatment results, the interaction detection results of population density, slope orientation with soil type, vegetation cover type, slope, DEM, average annual air temperature, average annual precipitation, land use type, and the gross regional product showed a two-factor enhancement. This result was different from other years. The interaction of the influence factor of population density with other elements on NDVI showed a stronger correlation than in previous years. This can indicate that human activities will have a particular impact on vegetation, and the specific result of the effect needs to be verified by the factor detection module of the Geodetector.

Table 5. Results of interactive detection in 2000.

	X1	X2	X3	X4	X5	X6	X7	X8	X9	X10
X1	0.587									
X2	0.704	0.457								
X3	0.609	0.496	0.159							
X4	0.602	0.469	0.181	0.004						
X5	0.697	0.626	0.565	0.496	0.484					
X6	0.698	0.603	0.529	0.435	0.530	0.423				
X7	0.666	0.676	0.557	0.549	0.698	0.659	0.535			
X8	0.679	0.568	0.466	0.440	0.607	0.594	0.661	0.430		
X9	0.666	0.647	0.479	0.414	0.678	0.689	0.679	0.632	0.403	
X10	0.589	0.473	0.184	0.026	0.488	0.426	0.537	0.437	0.413	0.016

The calculation results of the annual mean values from 1998 to 2019 differ from those of 2000, 2005, and 2010. The interaction detection between aspect and population density shows a non-linear enhancement. Population density is one of the most representative data points that responds to human activities visually. Therefore, this result also indicates that human factors have a role in influencing vegetation growth for NDVI values.

3.4.2. Ecological Analysis

Ecological detection results can detect whether there is a significant difference in the impact of various factors on the NDVI. The survey results in 2000 showed no significant difference in the effect of slope and population, average annual air temperature and land use type, and average annual air temperature and regional gross domestic product on the NDVI, while other factors have significant differences in NDVI values. The detection results in 2005, 2010, and 2015 showed that there was no significant difference between vegetation cover type and DEM, vegetation cover type and average annual precipitation, vegetation cover type and land use type, aspect and population density, DEM and average annual precipitation, and average annual air temperature and land use type in terms of their effect on NDVI values.

The ecological detection results of the annual mean values from 1998 to 2019 are shown in Table 6. There is no significant effect of slope and population density, average annual air temperature, and land use on NDVI values. The results of the ecological analysis show that vegetation cover type, slope, aspect, DEM, average annual air temperature, average annual precipitation, population density, and land use significantly affect NDVI values in the TAR, and there is no significant difference in the impact.

Table 6. Annual mean ecological detection results.

	X1	X2	X3	X4	X5	X6	X7	X8	X9	X10
X1										
X2	Y									
X3	Y	Y								
X4	Y	Y	Y							
X5	Y	Y	Y	Y						
X6	Y	Y	Y	Y	Y					
X7	Y	Y	Y	Y	Y	Y				
X8	Y	Y	Y	Y	Y	N	Y			
X9	Y	Y	Y	Y	Y	Y	Y	Y		
X10	Y	Y	Y	N	Y	Y	Y	Y	Y	

Note: Y indicates a significant difference in the effect of the two areas on vegetation NDVI, while N indicates no significant difference (F-test at 95% confidence level).

3.4.3. Factor Analysis

As shown in Table 7, the magnitude of the influence of each factor on the NDVI in the TAR in 2000 is as follows: soil type > average annual precipitation > DEM > vegetation cover type > land use type > average annual air temperature > gross regional product > slope > population density > aspect. The factor detection results of annual average values in 2005, 2010, and 2015, as well as from 1998 to 2019, all point to soil type having the most significant influence on NDVI values in the TAR; the effect of aspect on NDVI values is insignificant. The results of factor detection indicate that aspect and population density as single factors do not have a significant impact on the NDVI in the TAR; soil type and average annual precipitation as single factors are essential for studying the NDVI in the TAR.

Table 7. Factor detection results in 2000 (a) and 2005 (b) and mean annual values (c).

a	X1	X2	X3	X4	X5	X6	X7	X8	X9	X10
q	0.587	0.457	0.159	0.004	0.484	0.423	0.535	0.430	0.403	0.016
p	0.000	0.000	0.000	0.159	0.000	0.000	0.000	0.000	0.000	0.000
b	X1	X2	X3	X4	X5	X6	X7	X8	X9	X10
q	0.581	0.473	0.171	0.004	0.477	0.446	0.492	0.449	0.337	0.018
p	0.000	0.000	0.000	0.157	0.000	0.000	0.000	0.000	0.000	0.007
c	X1	X2	X3	X4	X5	X6	X7	X8	X9	X10
q	0.576	0.458	0.153	0.002	0.475	0.445	0.539	0.441	0.222	0.013
p	0.000	0.000	0.000	0.019	0.000	0.000	0.000	0.000	0.000	0.000

3.4.4. Risk Analysis

The results of the risk detection can provide some reference value for ecological conservation and vegetation restoration projects in the TAR. The suitable range or type of factors is crucial for vegetation growth. The results of risk detection in the Geodetector can be used to determine the content or type of elements suitable for vegetation growth. Therefore, risk detection is used to explore areas with better vegetation growth in the TAR. The basis of its interpretation is that the more significant the NDVI value, the better the vegetation growth.

Risk Detection of Average Annual Precipitation

The results of both the factor and ecological surveys indicate that average annual precipitation is one of the most critical factors influencing NDVI values in the TAR. The precipitation interval most suitable for vegetation growth in the TAR can be derived through risk detection, thus providing a valuable reference basis for vegetation conservation. As shown in Table 8, the spatial distribution of vegetation cover in the TAR is consistent with the spatial distribution of average annual precipitation. According to the natural intermittent point classification, the average annual precipitation was divided into nine subzones. The mean NDVI values usually increase with the increase in average annual precipitation. They peaked in the area with the highest average annual precipitation, thus indicating that precipitation promoted vegetation growth. The results showed that the NDVI values of average annual precipitation subzone nine significantly differed from other subzones. Therefore, the best vegetation cover was found in the range of 2840–3685 mm of average annual precipitation in the TAR from 1998 to 2019.

Table 8. Average annual precipitation risk detection results.

	1	2	3	4	5	6	7	8	9
1									
2	Y								
3	Y	Y							
4	Y	Y	Y						
5	Y	Y	Y	Y					
6	Y	Y	Y	Y	N				
7	Y	Y	Y	Y	Y	Y			
8	Y	Y	Y	Y	Y	Y	Y		
9	Y	Y	Y	Y	Y	Y	Y	Y	
NDVI	0.174	0.247	0.356	0.514	0.432	0.459	0.578	0.806	0.902

Note: Y indicates a significant difference in the effect of two areas on vegetation NDVI, while N indicates no significant difference (confidence level is 95% F-test); numbers 1–9 indicate 97–294, 294–519, 519–758, 758–997, 997–1306, 1306–1771, 1771–2305, 2305–2840, and 2840–3684, respectively (unit: mm).

Risk Detection of Average Annual Air Temperature

In the experiment, average annual air temperature significantly affected the NDVI in both interaction and factor detection. The interaction between average annual air temperature and other factors on the NDVI in the TAR showed a two-factor enhancement or non-linear enhancement trend. The results of risk detection show that NDVI values increase with increasing average annual air temperature and that the highest NDVI values are found in areas with the highest average annual air temperature, i.e., areas with better vegetation cover. It is clear from Table 9 that NDVI values in the TAR increase with increasing average annual air temperature and show a strong correlation with average annual air temperature.

Table 9. Average annual air temperature risk detection results.

	1	2	3	4	5	6	7	8	9
1									
2	Y								
3	Y	Y							
4	Y	Y	Y						
5	Y	Y	Y	Y					
6	Y	Y	Y	Y	Y				
7	Y	Y	Y	Y	Y	Y			
8	Y	Y	Y	Y	Y	Y	Y		
9	Y	Y	Y	Y	Y	Y	Y	Y	
NDVI	0.169	0.188	0.235	0.339	0.384	0.415	0.617	0.873	0.92

The risk detection results of air temperature in 2005, 2010, and 2015 showed that the higher the average annual air temperature, the higher the NDVI value, indicating a positive correlation between air temperature and vegetation growth. The combined factor, interaction, ecological, and risk detection results show that the interaction between air temperature and other factors will further affect vegetation cover in the TAR.

Risk Detection of Soil Types

The results of the factor detection of soil type show that NDVI values in the TAR significantly influence soil type (Table 10). At the same time, the interaction of soil type with other factors enhances its impact on the NDVI. The results of the risk detection show that red soils have a relatively significant effect on vegetation growth, with an NDVI value of 0.904 in the red soil-covered area. Yellow-brown and swampy soils have a lower impact on vegetation growth, with NDVI values of 0.751 and 0.728 in this covered area. The NDVI values in the mountainous scrub-steppe soil, glacier, and snow-covered regions are significantly lower than elsewhere. There were no significant differences in the effects of

yellow-brown and boggy soils on NDVI, nor were there differences for glaciers, snow cover, or lakes in terms of their effect on NDVI.

Table 10. Soil type risk detection results.

	1	2	3	4	5	6	7	8	9
1									
2	Y								
3	Y	N							
4	Y	Y	Y						
5	Y	Y	Y	Y					
6	Y	Y	Y	Y	Y				
7	Y	Y	Y	Y	Y	Y			
8	Y	Y	Y	Y	Y	Y	Y		
9	Y	Y	Y	Y	Y	Y	Y	N	
NDVI	0.904	0.728	0.751	0.327	0.603	0.359	0.469	0.241	0.239

Note: Y indicates a significant difference in the effect of NDVI on vegetation between the two areas, while N indicates no significant difference (confidence level of 95%); numbers 1–9 indicate red soil, yellow-brown soil, bog soil, mountain scrub soil, subalpine soil, alpine desert soil, glacial and snow cover, and lakes, respectively.

Risk Detection of Vegetation Cover Types

Vegetation cover type is an essential factor affecting the NDVI index in the TAR (Table 11). Their risk detection results show that the NDVI value of evergreen forests (0.873) is significantly higher than the NDVI value of other vegetation cover types. Broadleaf evergreen forests, evergreen coniferous forests, deciduous broadleaf forests, and deciduous coniferous forests are located in areas with better vegetation cover. There were no significant differences in NDVI between dryland, agricultural land, and other vegetation cover types or between bare ground and water and ice cover.

Table 11. Vegetation cover type risk detection results.

	1	2	3	4	5	6	7	8	9
1									
2	N								
3	Y	Y							
4	Y	Y	Y						
5	Y	Y	Y	Y					
6	Y	N	Y	Y	Y				
7	Y	Y	Y	Y	Y	Y			
8	Y	Y	Y	Y	Y	Y	Y		
9	Y	Y	Y	Y	N	Y	Y	Y	
NDVI	0.577	0.486	0.872	0.773	0.294	0.383	0.148	0.215	0.250

Note: Y indicates a significant difference in the effect of NDVI between the two areas, while N indicates no significant difference (confidence level 95%); numbers 1–9 indicate dryland, agricultural land, evergreen forest, deciduous forest, shrubland, grassland, bare land, water cover, and ice cover, respectively.

Risk Detection of Elevation

Altitude strongly correlates with human activity, plant growth conditions, and air temperature (Table 12). The risk detection results for altitude show that altitude significantly affects NDVI values in the TAR. The higher the altitude, the lower the NDVI values. The best vegetation growth was found in areas with altitudes of −304–1274 m in the TAR, while areas with altitudes above 4818 m had poor or no vegetation cover.

Table 12. Elevation risk detection results.

	1	2	3	4	5	6	7	8	9
1									
2	Y								
3	Y	Y							
4	Y	Y	Y						
5	Y	Y	Y	Y					
6	Y	Y	Y	Y	Y				
7	Y	Y	Y	Y	Y	Y			
8	Y	Y	Y	Y	Y	Y	Y		
9	Y	Y	Y	Y	Y	Y	Y	Y	
NDVI	0.92	0.904	0.837	0.645	0.528	0.365	0.279	0.253	0.182

Note: Y indicates a significant difference in the effect of two regions on NDVI, while N indicates no significant difference (confidence level 95%); numbers 1–9 indicate –304–1274, 1274–2351, 2351–3324, 3324–4030, 4030–4486, 4486–4818, 4818–5117, 5117–5483, and 5483–8824, respectively (unit: m).

Risk Detection of Land Use Types

There was a high spatial correlation between land use types and NDVI values. Woodlands (woodland, shrubland, open woodland) had the highest NDVI values. In contrast, the forest was not significantly different from agricultural land (dryland, paddy field), other woodland, and high-cover grassland but was very different from other land use types. Therefore, forest land, agricultural land, and high-cover gardens have the best vegetation cover. The land use types in the TAR are dominated by medium- and low-coverage grassland and bare rock and stone land, accounting for 63.5% of total land use, of which low-coverage grassland accounts for 51.7%. The second is unused land, accounting for 14.7%. From 1998 to 2015, the area of forest land and grassland in the TAR decreased, and the area of arable land, lakes, and saline land increased; however, the size of the change (region) was small and had little impact on the overall NDVI value in the TAR. Forest land, cultivated land, and construction land account for a small proportion of the total area of the TAR and are distributed in the central and high vegetation coverage areas in the east and south of the study area. The climate conditions in this area are good, and the precipitation is sufficient and suitable for human life and crop planting. The vegetation coverage is good, and the NDVI value is high.

Based on the results of this ecological exploration experiment (Tables 13 and 14), it can be found that the NDVI values of red soil, evergreen broad-leaved forest, evergreen coniferous forest, areas with a slope more significant than 25°, areas on a northern slope, and areas with an elevation of –304–1274 m are the highest, indicating that the vegetation growth of this suitable range or type is higher than that of other areas. At the same time, the higher the average annual precipitation and the higher the average annual air temperature, the higher the NDVI value. The correlation between GDP and population density and the NDVI of the TAR is low.

Table 13. Suitable range or types of natural factors in 2000.

Factor	Suitable Range or Type	NDVI Values
Soil type	Red soil	0.867
Type of vegetation cover	Evergreen broad-leaved forest, evergreen coniferous forest	0.851
Slope	>25°	0.720
Aspect	North	0.376
DEM	–304–1274 m	0.920
Average annual air temperature	15–24 °C	0.920
Average annual precipitation	2840–3685 mm	0.901
Land use type	Woodland	0.786
Gross regional product	Relatively high areas	0.646
Population density	Relatively high areas	0.600

Table 14. Suitable range or types of natural factors in terms of mean annual values.

Factor	Suitable Range or Type		
	2005	2010	2015
Soil type	Red Soil	Red Soil	Red Soil
Type of vegetation cover	Evergreen broad-leaved and coniferous forests	Evergreen broad-leaved and coniferous forests	Evergreen broad-leaved and coniferous forests
Slope	>25°	>25°	>25°
Aspect	North	North	North
DEM	−304–1274 m	−304–1274 m	−304–1274 m
Average annual air temperature	15.8–24.7 °C	16.5–25.3 °C	15.6–24.4 °C
Average annual precipitation	2746–3367 mm	3194–3845 mm	2762–3191 mm
Land use type	Woodland	Woodland	Woodland

Synergy of Other Factors

The Geodetector results of the geo-probe show that single factors such as slope, aspect, gross regional product, and population density have less influence on NDVI changes in the TAR. Nevertheless, the interaction between these factors will enhance the impact of NDVI changes.

The TAR has a vast territory and a large span, and the area is mainly composed of high mountains and steep mountains. The slope types are divided into nine subzones (0–5, 5–12, 12–17, 17–25, 25–30, 30–37, 37–45, 45–58, 58–89 (unit: °)). The higher the slope, the lower the significance of the effect on the NDVI. A slope below 25° significantly impacts NDVI values, and there is a substantial difference between areas with a gradient above 25° and those with a slope below 25°. There is no significant linear correlation between the changing slope trend and NDVI values, so slope has little impact on NDVI in the TAR. In the risk detection of aspect, we can see that the influence of aspect on NDVI values is insignificant. The highest NDVI values are found in the north tip of the aspect, so it can be judged that the vegetation cover of the north aspect is better compared to other regions.

The results of ecological detection for gross regional product reveal that the higher the gross regional product, the higher the NDVI value. The ecological detection results of population density are consistent with the regional gross domestic product. We have investigated the population of the TAR over the years and found that the overall population of the TAR increased slowly from 2000 to 2015. The apparent growth area is located in Lhasa, the provincial capital of the TAR. The trend in the NDVI shows that the NDVI values in and around Lhasa city have increased relative to the NDVI values in 2000, though the magnitude of the change in NDVI is insignificant. The NDVI values in the southern and southeastern TAR have changed significantly, but population density and regional GDP growth are negligible. Therefore, population density and regional GDP have no significant impact on the NDVI of the TAR.

At the same time, the result of factor detection also shows that the impact of population density on the NDVI value of the TAR is relatively low. According to analysis of population density data, the population density of the TAR is generally low, with a population density of 1500 (people/km²) accounting for more than 80% of the total area; most of the densely populated areas are distributed in Lhasa, Linzhi, Shannan, and Changdu. Air temperature, precipitation, and other factors in these areas suggest that these areas are most suitable for human life in the TAR, so it is difficult to explain the impact of population density on the NDVI value of the TAR as a single factor. If this area is not considered, the NDVI will first increase and then decrease with the increase in population density (for example, coastal regions or areas with highly concentrated economies).

4. Discussion

In the past few decades, under the influence of human activities and climate change, vegetation coverage in most regions of China has gradually increased [10], especially in northern areas such as Inner Mongolia and Xinjiang [31,32]. In the experiment, we selected long time series NDVI data. Through the combination of multiple factors and a comprehensive comparison of various methods, the experimental results are consistent with the changing trend of NDVI in China. This result shows that vegetation in the TAR grew well from 1998 to 2019 and that our experimental results are accurate.

In this study, we used the F-significance test and the Hurst index to analyze the vegetation change trend in the TAR from 1998 to 2019 and used the Hurst index to predict the future NDVI change trend in the TAR. Finally, we used four models of geographical exploration to analyze the driving factors and the interaction of elements of the NDVI in the TAR. In the following chapters, the research findings of this paper are discussed in detail.

4.1. Trend and Prediction Analysis of NDVI Changes

The study in this paper found that the vegetation index of the TAR has significant spatial differences. The regions with higher vegetation coverage in the TAR are Linzhi, Changdu, and Shannan. The central, northern, and western areas of the TAR have sparse vegetation coverage, and the distribution of NDVI is similar to the spatial distribution of air temperature and precipitation. This is relatively consistent with the research results of Feng et al. [17]. The results of the geographical detector also show that vegetation growth in the TAR is affected by both natural and human factors. Nevertheless, climate change is the main driving force of vegetation growth in the study area. The results of the F-significance test show that the changing trend of NDVI in the TAR from 1998 to 2019 shows an upward trend, with the increased part accounting for 72.56% of the total area of the autonomous region, which is consistent with the research results of Wu et al. [16]. The results show that vegetation coverage in the TAR is gradually increasing, and the vegetation growth status is good. The results of the F-significance test also showed that NDVI values in snow mountains and permanent ice cover areas showed a downward trend. Combined with the results of geographical detectors, we can see that the soil types and vegetation cover types in the study area have a significant impact on the intensity and direction of the NDVI change trend. At the same time, the spatial correlation is high, and the characteristics of NDVI changes in terms of the change in soil type and vegetation cover type are consistent with the research results of Sun [31] and Yang [32].

The results of related studies also show that current vegetation cover in the TAR is poor [33]. Therefore, with the help of the Hurst index, future vegetation growth can be predicted, and relative conservation measures can be made to develop vegetation. In this paper, the Hurst index showed that 72.06% of the area in the TAR showed an inverse trend in future vegetation growth, which is consistent with the results of Liu et al. [34]. In some regions of the Himalayas and Ali, the vegetation growth trend will decrease. Therefore, emphasis should be placed on protecting areas with low vegetation cover and areas where the Hurst index predicts a decrease. At the same time, the supervision and protection of areas prone to desertification and sandstorms should be increased.

4.2. Impact of Natural and Human Factors on NDVI

Climate change has a specific contribution to vegetation recovery [35]. Among the influencing factors selected for this experiment, the influence of precipitation on the NDVI in the TAR reached about 0.45, indicating that precipitation is one of the main factors influencing changes in vegetation growth in the TAR; NDVI values increased first and then started decreasing as average annual precipitation changes rose [10]. Additionally, intense precipitation can significantly affect changes in the spatial and temporal dimensions of the NDVI [36]. Yang et al. [37] suggested that air temperature was the main factor affecting the NDVI in the TAR compared to the effect of precipitation on the NDVI. This result may be due to the different time scales of the study and the various resolutions of the data used.

From 1998 to 2019, the TAR experienced higher air temperature changes than China [38] and lower precipitation than China [39]. The rapid increase in air temperature [40] and the relatively stable precipitation [41] in the TAR have led to regional warming and drought [42]. Some studies have shown that alpine meadows and grasslands strongly respond to precipitation [18]. In 2006, there was an extreme drought in the TAR that damaged pasture growth and destroyed grassland ecosystems, decreasing the NDVI [17]. As the NDVI has a lagging effect on precipitation [43], extreme weather in 2018 led to a sharp decrease in NDVI values in the autonomous region in 2019. Extreme precipitation events had a more pronounced effect on NDVI values than extreme air temperature events in the Tibetan Plateau region, indicating that vegetation is more sensitive to changes in precipitation. This study showed that the impact of precipitation on vegetation growth conditions was higher than that of air temperature on the NDVI, which is consistent with the findings of Ichii et al. [35]. This result will provide an essential basis for the study of vegetation cover in the TAR.

Elevation has an important influence on vegetation growth and human activities [44]. In the TAR, the topography is complex. The mountains are crisscrossed, with snow-capped mountains and ancient ice caps in some areas, which have apparent constraints on vegetation growth. The results of this experiment show that the influence of elevation on the NDVI is about 0.25, and the ecological environment is suitable in areas below 4000 m above sea level. The trend in vegetation cover with elevation changes first fluctuates upwards, then plateaus, and finally sharply decreases. This is similar to the findings of Li et al. [45].

Soil type is also an essential factor in determining the spatial variation of the NDVI [46]. Soil type not only affects the growth of plants but also limits vegetation's spatial distribution. In this experiment, soil type always appeared as the most influential factor in the results of each investigation. This is consistent with the findings of Xin et al. [47].

In this experiment, human factors had a weak influence on the NDVI, which is consistent with the results of Huang et al. [26]. This results from the fact that the TAR is sparsely populated [48] and that the water and heat conditions in most areas are not sufficient to supply vegetation growth and human life [49].

5. Summary and Conclusions

Using the NDVI, this study investigated the dynamic changes in vegetation in the TAR from 1998 to 2019. It analyzed the correlation between the NDVI and soil type, vegetation cover type, terrain factors (altitude, slope, and aspect), climate factors (air temperature and precipitation), and human activity factors (population density, gross regional product, land use type) using spatial trend analysis, F-significance tests, the Hurst index, and a geographic detector. The main conclusions are as follows:

(1) The areas with good vegetation cover in the TAR are the Linzhi, Lhasa, Shannan, and Changdu areas, and vegetation cover in Ali is the worst; the annual mean NDVI values of the TAR from 1998 to 2019 show an overall increasing trend, and the linear incremental rate for the mean NDVI value is 0.002/per year. The areas with severely degraded vegetation cover account for 1.95% of the total area, and areas with significant improvement account for 20.78%.

(2) The impact factors for NDVI in the TAR are ranked as follows: soil type > average annual precipitation > DEM > vegetation cover type > land use type > average annual air temperature > regional gross domestic product > slope > population density > aspect. The main driving factors are soil type, average annual precipitation, and DEM, with respective influences of about 0.58, 0.5, and 0.45.

(3) The influence factors for NDVI in the TAR in order of influence are as follows: soil type > average annual precipitation > DEM > vegetation cover type > land use type > average annual air temperature > gross regional product > slope > population density > aspect. The main driving factors are soil type, average annual precipitation, and DEM, with respective influences of about 0.58, 0.5, and 0.45.

This study not only presents the trends of NDVI mean values in the TAR for 22 years but also restores and predicts the past and future trends of the NDVI in space; meanwhile, it quantitatively describes the strength of each factor in explaining the spatial variation of the NDVI and provides a research direction for future vegetation protection in the TAR.

Author Contributions: J.W.: data curation, formal analysis, investigation, software, writing—original draft, writing—review and editing. J.Z.: resources, supervision, funding acquisition. P.Z.: conceptualization, methodology, resources, supervision, writing—review and editing, software, validation. K.L.: resources, supervision. Z.C.: formal analysis, visualization. H.Z.: validation, visualization. Y.H.: validation, visualization. Y.L.: formal analysis, validation. X.Y.: software, visualization. All authors have read and agreed to the published version of the manuscript.

Funding: This research was funded by the National Natural Science Foundation of China (Grant No. 41761081), the Basic Research Program of Yunnan Province (Grant No. 202201AU070112), the Kunming University of Science Technology introduced talent research start-up fund project (Grant No. KKZ3202021055), and the Yunnan Province Philosophy and Social Science Planning Project (Grant No. PY202129).

Data Availability Statement: Not applicable.

Acknowledgments: The authors would like to thank the researchers who provided the open-source algorithms, which were extremely helpful to the research conducted in this paper.

Conflicts of Interest: The authors declare no conflict of interest.

References

1. Zhou, P.; Zhao, D.; Liu, X.; Duo, L.; He, B. Dynamic Change of Vegetation Index and Its Influencing Factors in Alxa League in the Arid Area. *Front. Ecol. Evol.* **2022**, *10*. [[CrossRef](#)]
2. Wang, Z.; Lai, C.; Chen, X.; Yang, B.; Zhao, S.; Bai, X. Flood hazard risk assessment model based on random forest. *J. Hydrol.* **2015**, *527*, 1130–1141. [[CrossRef](#)]
3. Gong, C.; Tan, Q.; Liu, G.; Xu, M. Impacts of mixed forests on controlling soil erosion in China. *Catena* **2022**, *213*, 106147. [[CrossRef](#)]
4. Li, H.; Yan, Z.; Zhang, Z.; Lang, J.; Wang, X. A Numerical Study of the Effect of Vegetative Windbreak on Wind Erosion over Complex Terrain. *Forests* **2022**, *13*, 1072. [[CrossRef](#)]
5. Li, T.; Wang, Q.; Liu, Y.; Lai, C.; Lu, H.; Qiu, Y.; Tang, H. An exploration of sustainability versus productivity and ecological stability in planted and natural forests in Sichuan, China. *Land Degrad. Dev.* **2022**, *33*, 3641–3651. [[CrossRef](#)]
6. Boke-Olén, N.; Ardö, J.; Eklundh, L.; Holst, T.; Lehsten, V. Remotely sensed soil moisture to estimate savannah NDVI. *PLoS ONE* **2018**, *13*, e0200328. [[CrossRef](#)] [[PubMed](#)]
7. Xu, Y.; Yang, Y.; Chen, X.; Liu, Y. Bibliometric Analysis of Global NDVI Research Trends from 1985 to 2021. *Remote Sens.* **2022**, *14*, 3967. [[CrossRef](#)]
8. Ramírez-Cuesta, J.M.; Minacapilli, M.; Motisi, A.; Consoli, S.; Intrigliolo, D.S.; Vanella, D. Characterization of the main land processes occurring in Europe (2000–2018) through a MODIS NDVI seasonal parameter-based procedure. *Sci. Total Environ.* **2021**, *799*, 149346. [[CrossRef](#)]
9. Sharma, M.; Bangotra, P.; Gautam, A.S.; Gautam, S. Sensitivity of normalized difference vegetation index (NDVI) to land surface temperature, soil moisture and precipitation over district Gautam Buddh Nagar, UP, India. *Stoch. Environ. Res. Risk Assess.* **2022**, *36*, 1779–1789. [[CrossRef](#)]
10. Liu, Y.; Tian, J.; Liu, R.; Ding, L. Influences of Climate Change and Human Activities on NDVI Changes in China. *Remote Sens.* **2021**, *13*, 4326. [[CrossRef](#)]
11. Dai, Q.; Cui, C.; Wang, S. Spatiotemporal variation and sustainability of NDVI in the Yellow River basin. *Irrig. Drain.* **2022**, *71*, 1304–1318. [[CrossRef](#)]
12. Sajadi, P.; Sang, Y.; Gholamnia, M.; Bonafoni, S.; Brocca, L.; Pradhan, B.; Singh, A. Performance Evaluation of Long NDVI Timeseries from AVHRR, MODIS and Landsat Sensors over Landslide-Prone Locations in Qinghai-Tibetan Plateau. *Remote Sens.* **2021**, *13*, 3172. [[CrossRef](#)]
13. Wang, J.; Xu, D. Geodetector: Principle and prospective. *Acta Geogr. Sin.* **2017**, *72*, 116–134. (In Chinese)
14. Dong, Y.; Yin, D.; Li, X.; Huang, J.; Su, W.; Li, X.; Wang, H. Spatial-temporal evolution of vegetation NDVI in association with climatic, environmental and anthropogenic factors in the loess plateau, China during 2000–2015: Quantitative analysis based on geographical detector model. *Remote Sens.* **2021**, *13*, 4380. [[CrossRef](#)]
15. Gao, S.; Dong, G.; Jiang, X.; Nie, T.; Yin, H.; Guo, X. Quantification of Natural and Anthropogenic Driving Forces of Vegetation Changes in the Three-River Headwater Region during 1982–2015 Based on Geographical Detector Model. *Remote Sens.* **2021**, *13*, 4175. [[CrossRef](#)]

16. Wu, N.; Wang, Y.; Liu, Y.; Li, M. Spatial-temporal Changes of NDVI in the three northeast provinces and Its Dual Response to Climate Change and Human Activities. *Front. Environ. Sci.* **2022**, *1551*. [[CrossRef](#)]
17. Feng, J.; Zhang, K.; Chao, L.; Liu, L. An improved process-based evapotranspiration heat fluxes remote sensing algorithm based on the Bayesian and Sobol'uncertainty analysis framework using eddy covariance observations of Tibetan grasslands. *J. Hydrol.* **2022**, *613*, 128384. [[CrossRef](#)]
18. Liu, D.; Wang, T.; Yang, T.; Yan, Z.; Liu, Y.; Zhao, Y.; Piao, S. Deciphering impacts of climate extremes on Tibetan grasslands in the last fifteen years. *Sci. Bull.* **2019**, *64*, 446–454. [[CrossRef](#)]
19. Han, W.; Chen, D.; Li, H.; Chang, Z.; Chen, J.; Ye, L.; Wang, Z. Spatiotemporal Variation of NDVI in Anhui Province from 2001 to 2019 and Its Response to Climatic Factors. *Forests* **2022**, *13*, 1643. [[CrossRef](#)]
20. Zhang, Y.; He, Y.; Li, Y.; Jia, L. Spatiotemporal variation and driving forces of NDVI from 1982 to 2015 in the Qinba Mountains, China. *Environ. Sci. Pollut. Res.* **2022**, *29*, 52277–52288. [[CrossRef](#)]
21. Ogou, F.K.; Ojeh, V.N.; Naabil, E.; Mbah, C.I. Hydro-climatic and water availability changes and its relationship with NDVI in Northern Sub-Saharan Africa. *Earth Syst. Environ.* **2022**, *6*, 681–696. [[CrossRef](#)]
22. Nanzad, L.; Zhang, J.; Tuvdendorj, B.; Nabil, M.; Zhang, S.; Bai, Y. NDVI anomaly for drought monitoring and its correlation with climate factors over Mongolia from 2000 to 2016. *J. Arid. Environ.* **2019**, *164*, 69–77. [[CrossRef](#)]
23. Baniya, B.; Tang, Q.; Huang, Z.; Sun, S.; Techato, K.A. Spatial and temporal variation of NDVI in response to climate change and the implication for carbon dynamics in Nepal. *Forests* **2018**, *9*, 329. [[CrossRef](#)]
24. Ren, Z.; Tian, Z.; Wei, H.; Liu, Y.; Yu, Y. Spatiotemporal evolution and driving mechanisms of vegetation in the Yellow River Basin, China during 2000–2020. *Ecol. Indic.* **2022**, *138*. [[CrossRef](#)]
25. Mazzarino, M.; Finn, J.T. An NDVI analysis of vegetation trends in an Andean watershed. *Wetl. Ecol. Manag.* **2016**, *24*, 623–640. [[CrossRef](#)]
26. Huang, C.; Yang, Q.; Huang, W. Analysis of the Spatial and Temporal Changes of NDVI and Its Driving Factors in the Wei and Jing River Basins. *Int. J. Environ. Res. Public Health* **2021**, *18*, 11863. [[CrossRef](#)] [[PubMed](#)]
27. Ghebregabher, M.G.; Yang, T.; Yang, X.; Sereke, T.E. Assessment of NDVI variations in responses to climate change in the Horn of Africa. *Egypt. J. Remote Sens.* **2020**, *23*, 249–261. [[CrossRef](#)]
28. Xu, M.; Zhang, J.; Li, Z.; Mo, Y. Attribution analysis and multi-scenario prediction of NDVI drivers in the Xilin Gol grassland, China. *J. Arid. Land.* **2022**, *14*, 941–961. [[CrossRef](#)]
29. Gillespie, T.W.; Madson, A.; Cusack, C.F.; Xue, Y. Changes in NDVI and human population in protected areas on the Tibetan Plateau. *Arct. Antarct. Alp. Res.* **2019**, *51*, 428–439. [[CrossRef](#)]
30. Wei, Y.; Sun, S.; Liang, D.; Jia, Z. Spatial-temporal variations of NDVI and its response to climate in China from 2001 to 2020. *Int. J. Digit. Earth* **2022**, *15*, 1463–1484. [[CrossRef](#)]
31. Sun, R.; Chen, S.; Su, H. Climate dynamics of the spatiotemporal changes of vegetation NDVI in northern China from 1982 to 2015. *Remote Sens.* **2021**, *13*, 187. [[CrossRef](#)]
32. Yang, D.; Yi, G.; Zhang, T.; Li, J.; Qin, Y.; Wen, B.; Liu, Z. Spatiotemporal variation and driving factors of growing season NDVI in the Tibetan Plateau, China. *J. Appl. Ecol.* **2021**, *32*, 1361–1372.
33. Pan, S.; Zhao, X.; Yue, Y. Spatiotemporal changes of NDVI and correlation with meteorological factors in northern China from 1985–2015. *E3S Web Conf.* **2019**, *131*, 01040. [[CrossRef](#)]
34. Yuan, Z.; Yu, Z.; Feng, Z.; Xu, J.; Yin, J.; Yan, B.; Lei, H. Spatiotemporal Variations of NDVI in Terrestrial Ecosystem in Yangtze River Basin and Response to Hydrothermal Condition. *J. Yangtze River Sci. Res. Inst.* **2019**, *36*, 7.
35. Ichii, K.; Kawabata, A.; Yamaguchi, Y. Global correlation analysis for NDVI and climatic variables and NDVI trends: 1982–1990. *Int. J. Remote Sens.* **2002**, *23*, 3873–3878. [[CrossRef](#)]
36. Enebish, B.; Dashkhuu, D.; Renchin, M.; Russell, M.; Singh, P. Impact of Climate on the NDVI of Northern Mongolia. *J. Indian Soc. Remote* **2020**, *48*, 333–340. [[CrossRef](#)]
37. Sun, J.; Cheng, G.; Li, W.; Sha, Y.; Yang, Y. On the variation of NDVI with the principal climatic elements in the Tibetan Plateau. *Remote Sens.* **2013**, *5*, 1894–1911. [[CrossRef](#)]
38. Yang, K.; Guo, D.; Hua, W.; Pepin, N.; Yang, K.; Li, D. Tibetan plateau temperature extreme changes and their elevation dependency from ground-based observations. *J. Geophys. Res. Atmos.* **2022**, *127*, e2021JD035734. [[CrossRef](#)]
39. Li, X.; Wu, P.; Ding, Y.; Liu, Y.; Li, Q. Spatial-temporal variation of precipitation recycling over the Tibetan Plateau under climate warming. *Atmos. Res.* **2022**, *280*, 106431. [[CrossRef](#)]
40. Peng, X.; Frauenfeld, O.; Jin, H.; Du, R.; Qiao, L.; Zhao, Y.; Zhang, T. Assessment of temperature changes on the Tibetan Plateau during 1980–2018. *Earth Space Sci.* **2021**, *8*, e2020EA001609. [[CrossRef](#)]
41. Teng, K.; Cai, H.; Sun, X.; Chen, Q. Geometric and Physical Characteristics of Precipitation Clouds in Tibetan Plateau. *Adv. Meteorol.* **2022**, *2022*, 9181219. [[CrossRef](#)]
42. Chen, B.; Chen, H.; Li, M.; Fiedler, S.; Märgärint, M.C.; Nowak, A.; Wu, J. Climate Sensitivity of the Arid Scrublands on the Tibetan Plateau Mediated by Plant Nutrient Traits and Soil Nutrient Availability. *Remote Sens.* **2022**, *14*, 4601. [[CrossRef](#)]
43. Kundu, A.; Denis, D.M.; Patel, N.R.; Dutta, D. A Geo-spatial study for analysing temporal responses of NDVI to rainfall. *Singap. J. Trop. Geogr.* **2018**, *39*, 107–116. [[CrossRef](#)]
44. Riihimäki, H.; Heiskanen, J.; Luoto, M. The effect of topography on arctic-alpine aboveground biomass and NDVI patterns. *Int. J. Appl. Earth Obs.* **2017**, *56*, 44–53. [[CrossRef](#)]

45. Wang, Z.; Cao, S.; Cao, G. The Effect of Vegetative Coverage and Altitude on the Vegetation Water Consumption in the Alpine Inland River Basin of the Northeastern Qinghai–Tibet Plateau. *Water* **2022**, *14*, 1113. [[CrossRef](#)]
46. Nie, T.; Dong, G.; Jiang, X.; Lei, Y. Spatio-temporal changes and driving forces of vegetation coverage on the loess plateau of Northern Shaanxi. *Remote Sens.* **2021**, *13*, 613. [[CrossRef](#)]
47. Yan, X.; Wang, R.; Niu, Z. Response of China’s Wetland NDVI to Climate Changes. *Wetlands* **2022**, *42*, 1–14. [[CrossRef](#)]
48. Altieri, M.A.; Letourneau, D.K. Vegetation management and biological control in agroecosystems. *Crop. Prot.* **1982**, *1*, 405–430. [[CrossRef](#)]
49. Ding, Y.; Li, Z.; Peng, S. Global analysis of time-lag and-accumulation effects of climate on vegetation growth. *Int. J. Appl. Earth Obs.* **2020**, *92*, 102179. [[CrossRef](#)]

Disclaimer/Publisher’s Note: The statements, opinions and data contained in all publications are solely those of the individual author(s) and contributor(s) and not of MDPI and/or the editor(s). MDPI and/or the editor(s) disclaim responsibility for any injury to people or property resulting from any ideas, methods, instructions or products referred to in the content.